

Research Paper:

Dynamic Pattern Recognition Model Based on Neural Network Response to Signal Fluctuation

Hiroataka Doho*, Haruhiko Nishimura**, and Sou Nobukawa***

*Faculty of Education, Kochi University
2-5-1 Akebono-cho, Kochi 780-8520, Japan
E-mail: doho@kochi-u.ac.jp

**Graduate School of Applied Informatics, University of Hyogo
7-1-28 Minatojima-Minami-cho, Chuo-ku, Kobe, Hyogo 650-0047, Japan

***Department of Computer Science, Chiba Institute of Technology
2-17-1 Tsudanuma, Narashino, Chiba 275-0016, Japan

[Received July 21, 2020; accepted August 10, 2022]

We have proposed a model of dynamic retrieval in associative memory based on temporal input/output correlations under a stimulus-response open scheme of neural networks. This mechanism is different from that of the conventional stationary Hopfield model in which the input signal is used only as information for the initial state of the network. Building upon the fundamental properties of the proposed model, in this paper, we newly evaluate the dependence of identification performance on the signal fluctuation level and on the number of stored patterns by introducing an accuracy rate for known (stored) and unknown (non-stored) patterns, based on the network correlation to the input signal with fluctuation. The results indicate that the dynamic scheme of network response to a fluctuating signal leads to increased efficacy and usefulness.

Keywords: neural network, signal fluctuation, pattern recognition, associative memory, input/output correlation

1. Introduction

Associative memory neural networks, which were proposed by Hopfield [1, 2], introduced the concept of an energy function to neural networks, where the target pattern to be memorized is set at a local equilibrium state of the energy function. Furthermore, with a focus on its stability, the neural network systems have been applied not only to associative memory, but also to combinatorial optimization and other problems, and their use as engineering models has advanced considerably [3–7]. However, in this model, interaction with the outside of the network is limited to the acquisition of external information at the initial state, after which the network behaves as a closed system where state transitions follow a relaxation process of convergence toward a low-energy equilibrium point (point attractor). Then its applicable problems are limited as a model framework of memorization and retrieval.

In order to make a system behavior dynamic, stochastic neural networks and chaotic neural networks have been applied remaining the system closed [7–9]. However, a more realistic model can be obtained if the network is regarded as an open dynamic system in which external information operates on the network state in the form of a persistent input signal [10–14].

A mechanism for identification and discrimination of pattern information by using a dynamic memory model based on this extension has been proposed [15]. Specifically, external information, which is used to initialize the network state in the conventional model, is directly added over time to the internal state of the network as an external input term in the input-output system, and the effect of this term on the network is taken as a change in the internal state of each neuron. Therefore, the external input not only contains pattern information, but also has a certain signal strength, and the time series of pattern information can be added a certain fluctuation. Also, it is possible to realize the process of signal recognition by using input-output temporal correlation to evaluate the dynamic difference in the network response for the external input (input signal) corresponding to stored and non-stored patterns.

Thus far, aiming to construct the above-mentioned process of signal discrimination, we have investigated the fundamental properties of dynamic responsiveness of networks by starting with the dependence of the input-output temporal correlation on the signal strength and the switching interval of the signal fluctuation, as well as the influence of different settings for the basin of memory attraction [15, 16]. This scheme proposes a method to identify whether the input pattern is known or not, only by external observation of the input/output signal without directly accessing the internal dynamical structure of the neural network system such as the energy function. In this paper, we investigate the discrimination accuracy for stored and non-stored patterns depending on the fluctuation level of the input signal as well as on the number of stored patterns in detail. Consequently, we demonstrate the effectiveness of the dynamic discrimination model based on the differ-



ences in responsiveness of the neural network to signal fluctuation. We believe that this extension of the Hopfield model, a closed system, to an open system is the first step in introducing it to signal processing and identification in machine learning and artificial intelligence systems.

2. Modeling

2.1. Dynamic Memorization Model and Signal Discrimination Mechanism

We consider N neurons $\{X_i\}$ indexed by $i = 1, 2, \dots, N$ connected with synaptic weight w_{ij} between neurons i and j (if $i = j$ then $w_{ij} = 0$). In conventional static memory models based on associative memory neural networks [1], external information is used as the initial network state $X(0) \in \mathbb{R}^N$ at $t = 0$, and subsequently the temporal development for each neuron is given by

$$X_i(t+1) = f(h_i(t)) \quad . \quad . \quad . \quad . \quad . \quad . \quad . \quad . \quad . \quad (1)$$

and

$$h_i(t) = \sum_{j=1}^N w_{ij} X_j(t) - \theta_i. \quad . \quad . \quad . \quad . \quad . \quad . \quad . \quad . \quad (2)$$

Here, $f(y) = \tanh(y/2\epsilon)$, neuron value X_i is defined as $X_i \in [-1, 1]$, and θ_i is the threshold. The dynamics (stability) of discrete-time and continuous-state network dynamics is explained in detail in references [17, 18].

We extend this static memory model into a form that includes the capability to interact with its outside. Specifically, the contribution from external signals is in the form of external force terms $\{S_{iI}\}$ ($i = 1, \dots, N$) added to the internal state in Eq. (1) as follows:

$$X_i(t+1) = f(h_i(t) + S_i(t)). \quad . \quad . \quad . \quad . \quad . \quad . \quad . \quad (3)$$

In contrast to static memory models, which behave as closed systems, $\{S_i(t)\}$ and $\{X_i(t+1)\}$ have a mutual relation in the forms of input and output.

The following equation is the energy function of the network state $\mathbf{X} \in \mathbb{R}^N$.

$$E(\mathbf{X}) = -\frac{1}{2} \sum_{i,j=1}^N w_{ij} X_i X_j + \sum_{i=1}^N \theta_i X_i. \quad (4)$$

Here, j is also the index of N neurons ($j = 1, 2, \dots, N$). If we take $w_{ij} = w_{ji}$, then

$$\frac{\partial E(\mathbf{X})}{\partial X_i} = - \sum_{j=1}^N w_{ij} X_j(t) + \theta_i = -h_i(t) \quad . \quad . \quad . \quad (5)$$

and Eq. (3) becomes

$$X_i(t+1) = f\left(-\frac{\partial E(\mathbf{X})}{\partial X_i} + S_i(t)\right). \quad (6)$$

In a system depending on external input, $E(X)$ is not an energy function in a strict sense. However, we refer to it as an energy function for its analogy with the static memory model.

At this stage, the following properties are revealed

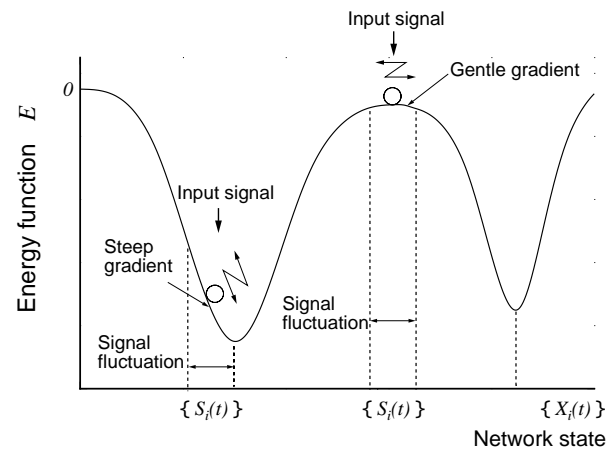


Fig. 1. Scheme of dynamic associative model.

upon extending the static model to an input/output system. When an input signal is applied, the network is influenced both by the force $S_i(t)$ of the input signal and the attractive force $-\partial E(X)/\partial X_i$ associated with the gradient of the energy function corresponding to the network state, and the behavior of the network depends on the competition between these two factors. In other words, as shown in **Fig. 1**, if a signal that is similar to a stored (memorized) pattern is applied, the network state is led into the vicinity of a corresponding local equilibrium state, where the influence of the input signal is weakened due to the large gradient of the energy function. On the other hand, if the applied input signal does not resemble any of the memorized patterns, the gradient of the energy function in the state into which the network is led is small, and the influence of the input signal becomes dominant. This difference is reflected in the changes in the network state over time in response to the input signal. In addition, it is expected that changes in the network state will be even more pronounced if fluctuation (noise fluctuating within a given interval) is assigned to the signal. Our dynamic memory model is capable of distinguishing between stored and non-stored pattern signals by focusing on such changes in the responsiveness of the network.

2.2. Learning Rule for Pattern Memorization

Pattern memorization is done by embedding of stationary patterns into conventional static memory models. Let μ be the index of stored patterns and M be the total number of stored patterns ($\mu = 1, \dots, M$). It is known that the necessary and sufficient condition for a pattern R^μ with components ξ_i^μ ($i = 1, \dots, N$) to match a local equilibrium of the network (i.e., $\{X_i(t+1)\} = \{X_i(t)\} = \{\xi_i^\mu\}$) is that the following holds [4]:

 $\forall i = 1, 2, \dots, N, \kappa > 0$ satisfying

$$\gamma_i^\mu \equiv \xi_i^\mu \sum_{j=1}^N w_{ij} \xi_j^\mu > \kappa. \quad (7)$$

By introducing the positive parameter κ , a basin of attraction is created with a locally stable $\{\xi_i^\mu\}$, and the network

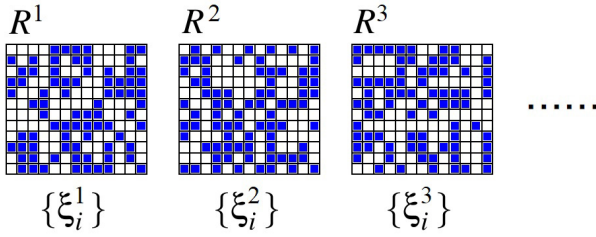


Fig. 2. Examples of random patterns (white and black pixels represent $\xi_i = -1$ and $+1$, respectively).

state $\{X_i(t)\}$ eventually becomes $\{\xi_i^\mu\}$, even if the memorized pattern $\{\xi_i^\mu\}$ is somewhat displaced.

In this regard, γ_i^μ is referred to as the stability level of memorization. κ which is the lower limit of γ_i^μ is referred to as the attraction basin parameter.

Diederich and Oppel [19] proposed a sequential learning rule (referred to as the iterative learning rule below) which slowly changes the connection weights in accordance with

$$w_{ij}^{\text{new}} = w_{ij}^{\text{old}} + \delta w_{ij}^\mu \quad \left(\delta w_{ij}^\mu = \frac{c}{N} \xi_i^\mu \xi_j^\mu \right) \quad . \quad (8)$$

until Eq. (7) is fulfilled with respect to M given memorized patterns, and its convergence has been proved. Here, c is a coefficient assigned in the process of memorization. By using this method, non-orthogonal pattern groups which are mutually correlated similarly to ordinary character patterns can also be represented in the network as local equilibrium states. If the objects of memorization are orthogonal pattern groups, this learning rule is reduced to the well-known Hebb rule [20].

3. Simulation Setup

3.1. Generation of Pattern Data and Stored Patterns

In the experiments, the number of neurons constituting the network was set to 156 ($N = 156$), the neuron threshold was taken as $\{\theta_i\} = 0$, and the slope of the input/output function was taken as $\varepsilon = 0.015$. In terms of pattern information, we prepared 50 random patterns (R^1, R^2, \dots, R^{50}) composed of $12 \times 13 (= 156)$ unit structures, as shown in **Fig. 2**. In these patterns, half of the units were $\xi_i = 1$ and the other half were $\xi_i = -1$, and the overlap $q_{\mu\nu} \equiv (1/N) \sum_{i=1}^N \xi_i^\mu \xi_i^\nu$ between R^1, R^2, \dots, R^{50} was distributed in $[-0.24, 0.26]$.

With R^1, \dots, R^{20} taken as stored pattern targets, **Fig. 3** presents the count distribution of the stability γ_i^μ ($156 \times 20 = 3120$) after memorization (interval width $\Delta\gamma_i^\mu = 0.05$) conducted under the condition of $2.0 < \gamma_i^\mu \leq 3.0$ of the iterative learning rule and the coefficient assigned in the process of memorization $c = 0.5$ explained in Section 2.2.

Figure 4 presents the energy value E calculated for the state of each pattern on the basis of post-memorization

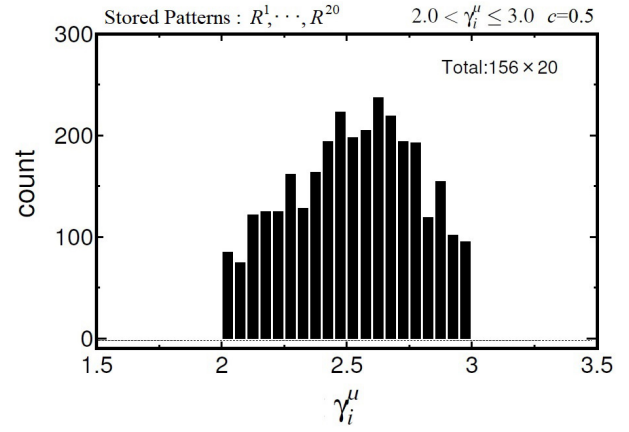


Fig. 3. Distribution of stability level after iterative learning for R^1, \dots, R^{20} under the condition of $2.0 < \gamma_i^\mu \leq 3.0$ and $c = 0.5$ (c is introduced in Eq. (8)).

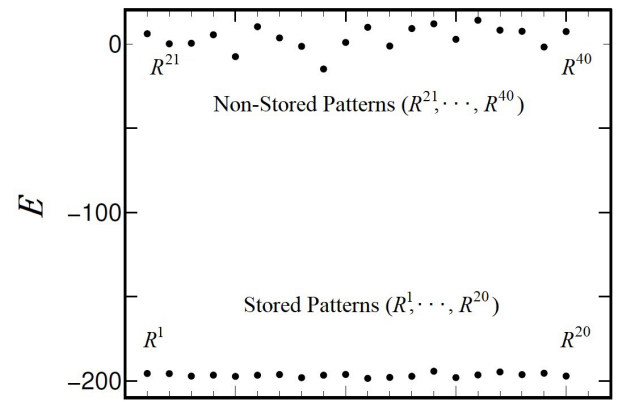


Fig. 4. Comparison of the energy function values between stored patterns R^1, \dots, R^{20} and non-stored patterns R^{21}, \dots, R^{40} .

connection weights $\{w_{ij}\}$. Although the energy of all 20 patterns R^1, \dots, R^{20} memorized in the network is low (around -200), the energy for the 20 patterns R^{21}, \dots, R^{40} which were not memorized (referred to as non-stored patterns below) is around 0 (± 15). Considering Eq. (7) in regard to Eq. (4), the energy corresponding to each of the pattern states $\{\xi_i^\mu\}$ becomes $E^{(\mu)} = -(1/2) \sum_{i,j} w_{ij} \xi_i^\mu \xi_j^\mu = -(1/2) \sum_{i=1}^N \gamma_i^\mu$, and by using the fact that the mean value of γ_i^μ for stored patterns is about 2.5 from **Fig. 3**, we obtain $E^{(\mu)} \simeq -(1/2) \times N \times 2.5 = -(1/2) \times 156 \times 2.5 = -195$.

3.2. Method for Evaluating Network Response

We prepare input signals by assigning a certain fluctuation to a pattern. Details about the procedure for generating fluctuation are given below. Several of the 156 elements constituting pattern R^μ (the elements are denoted as $\{\xi_i^\mu\}$) are extracted at random and inverted ($1 \rightarrow -1$, $-1 \rightarrow 1$). The number of extracted elements in this case is determined in accordance with a set fluctuation level.

The fluctuation level (F_L) indicates the maximum allowed number of extracted elements:

$$F_L = \frac{2h}{N}, \dots \dots \dots (9)$$

where h is the maximum allowed number of extracted elements. $F_L = 1$ corresponds to 78 elements (half of the total number N), while $F_L = 0$ corresponds to 0 elements. For example, if $F_L = 0.4$, the number of inverted elements is in the range of 0 to 31 since $(N/2) \times 0.4 = 78 \times 0.4 \approx 31$. By randomly inverting the target elements within each switching time interval (T_I), we make an information train $\{\xi_i^\mu\}_{F_L}^{T_I}$ that is maintained over time. Time interval T_I is set to be constant. For example, $\{\xi_i^\mu\}_{F_L=0.4}^{T_I} = [\{\xi_{i(0.04)}^\mu\} \rightarrow \{\xi_{i(0.16)}^\mu\} \rightarrow \{\xi_{i(0)}^\mu\} \rightarrow \{\xi_{i(0.28)}^\mu\} \rightarrow \dots]$, given with a change in the fluctuation value z at each T_I . Here, z for each $\{\xi_{i(z)}^\mu\}$ is the fluctuation randomly set during each T_I within the range 0 to 0.4, and when the number of inversions is a , a is given as $a = \operatorname{argmin}_{a' \in \mathbb{N}} \{|a' - 78z|\}$. The input signals are constructed as

$$\{S_i\}^{T_I} = s\{\xi_i^\mu\}_{F_L}^{T_I} \dots \dots \dots (10)$$

by multiplying the above-mentioned input information $\{\xi_i^\mu\}_{F_L}^{T_I}$ with a parameter s (referred to as signal strength).

In performing quantitative evaluation of the network response to these input signals, the input signal at each moment, as well as the corresponding network state, are regarded as N -dimensional vectors, and the following temporal correlations are introduced between these two vectors [14]. If the vectors for the input signal $\{S_i(t)\}$ and its corresponding network state $\{X_i(t)\}$ (referred to as network output below) are denoted as $\tilde{S}(t) = (S_1(t), S_2(t), \dots, S_N(t))$ and $X(t) = (X_1(t), X_2(t), \dots, X_N(t))$, the temporal correlation r is defined as

$$r = \frac{C(\tilde{S}(t), X(t+1))}{\sqrt{C(\tilde{S}(t), \tilde{S}(t))} \cdot \sqrt{C(X(t+1), X(t+1))}} \dots \dots (11)$$

Here, $C(Y, Z) = \overline{(Y - \bar{Y}) \cdot (Z - \bar{Z})}$, \bar{Y} and \bar{Z} indicate averaging Y and Z over time, and $\tilde{S} = S/s$. r is in the interval between -1 and $+1$, and in case the value is closer to $+1$, it is considered that the network output follows the fluctuating input signal well. By using r , the network responsiveness in the dynamic memory model can be evaluated by varying the signal strength s .

4. Simulation Results

4.1. Input Pattern Signals and Network Response

First, we conducted an analysis with respect to stored pattern signals and non-stored pattern signals by setting $F_L = 0.4$ and $T_I = 1$. **Fig. 5** contains a three-dimensional representation of the temporal changes of the input information $\tilde{S}(t) = \{\xi_i^1(t)\}_{F_L}, \{\xi_i^{34}(t)\}_{F_L}$ when R^1 is used as a stored pattern and R^{34} is used as a non-stored pattern, by

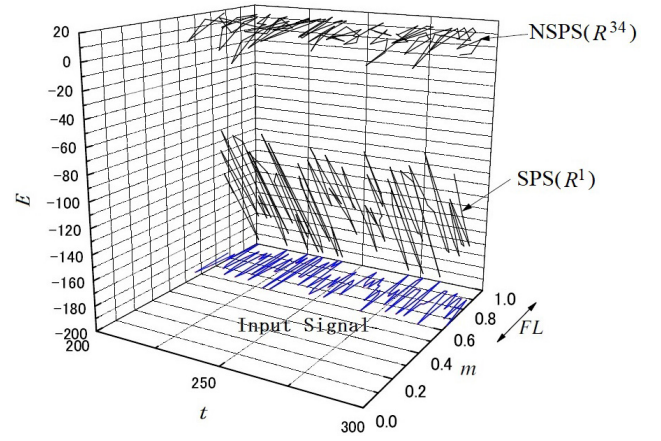


Fig. 5. Time series of stored pattern input signal (SPS) and non-stored pattern input ones (NSPS) with the same fluctuation $F_L = 0.4$, shown by the energy function and the overlaps m .

using the following overlaps between the input patterns with and without fluctuation

$$m_l^\mu(t) = \frac{1}{N} \sum_{i=1}^N \tilde{S}_i(t) \xi_i^\mu = \frac{1}{N} \tilde{S}(t) \cdot \xi^\mu \dots \dots (12)$$

and the corresponding energy $E(\tilde{S}(t))$. The projection onto the m - t plane corresponds to the time series $m_l^1(t)$ and $m_l^{34}(t)$ of Eq. (12). The respective overlaps corresponding to the patterns R^1 and R^{34} in $\tilde{S}(t)$ coincides each other ($m_l^1(t) = m_l^{34}(t)$), because the method for generating fluctuation is the same. Nevertheless, there is a remarkable difference between the energy value corresponding to a stored pattern (R^1) and that for a non-stored pattern (R^{34}). Namely, the energy for a non-stored pattern is around 0, whereas that for a stored pattern takes a value in the wide interval between -200 and -80 . The fact that such a difference exists between the two patterns even though the fluctuation level is the same is attributed to the different gradient of the energy function as shown in **Fig. 1** in Section 2.1. This can also be confirmed from **Fig. 6**, which shows the relation between the overlaps m_l^μ and the energy E of the input information for each pattern. Since there are multiple input information states with the same values of m^μ , the corresponding energy values become zoned. The case of $F_L = 0.4$ with $z = 0$ to 0.4 corresponds to a gradient difference in the interval of $0.6 < m^\mu < 1.0$.

The overlaps between the network output $X(t)$ and the pattern information $\{\xi_i^\mu\}$ is given by

$$m_o^\mu(t) = \frac{1}{N} X(t) \cdot \xi^\mu \dots \dots \dots (13)$$

Figure 7 shows $m_o^\mu(t)$ and $E(X(t))$ for the network output $\{X_i(t)\}$ in the case with signal strength $s = 2.25$, together with the input information from **Fig. 5** (represented with a broken line). Since the energy displacement in the case of a non-stored pattern signal is small, the network output is almost the same as that for the non-stored pat-

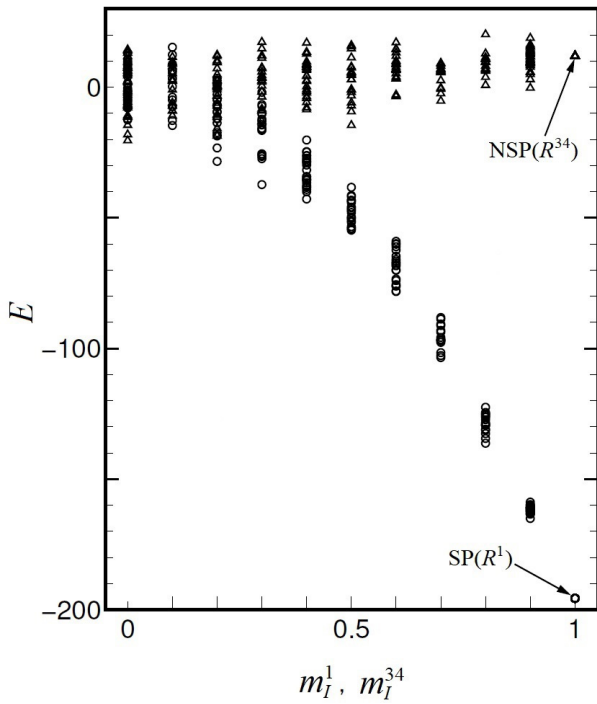


Fig. 6. Slopes of the energy function obtained by changing the overlap state for stored patterns (SP) and non-stored patterns (NSP).

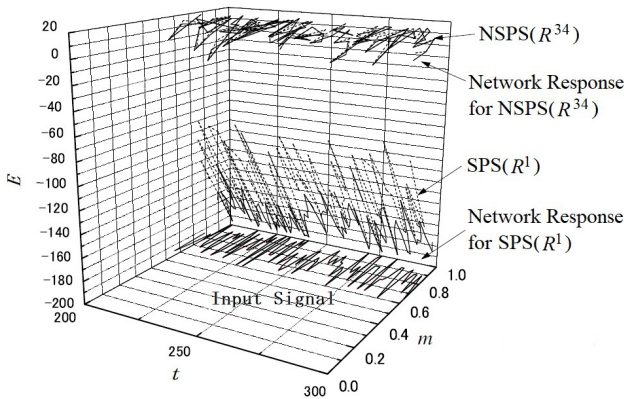


Fig. 7. Time series of network responses to SPS and NSPS when $s = 2.25$.

tern signal (R^{34}) in **Fig. 5**. On the other hand, the energy displacement in the case of a stored pattern signal is large, and the network output does not follow the case of a stored pattern signal (R^1) in **Fig. 5**. In evaluating the difference between the two network responses by using the temporal correlation in Eq. (11), we obtain $r = 0.646$ in the case of a stored pattern signal (R^1) and $r = 0.979$ in the case of non-stored pattern signal (R^{34}).

4.2. Dependence of Network Response on Signal Strength

Next, we calculated the temporal correlation r for each time series obtained for different values of s as in the case of **Fig. 7** (up to $t = 1000$; the step size of s in the simula-

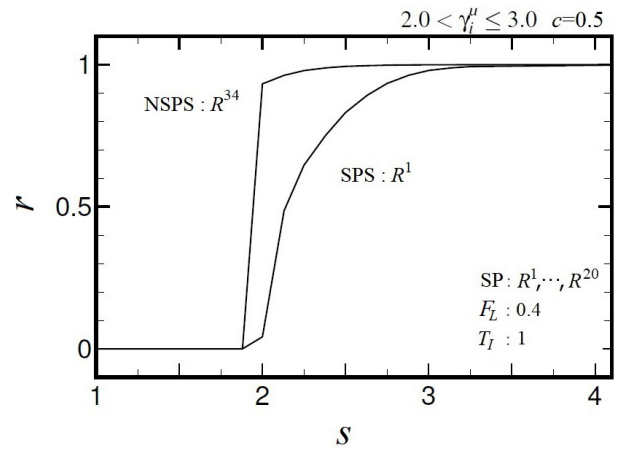


Fig. 8. Dependence of network response on signal strength when the number of stored patterns $M = 20$, $F_L = 0.4$ and $T_I = 1$ under the condition of $2.0 < \gamma_i^\mu \leq 3.0$ and $c = 0.5$.

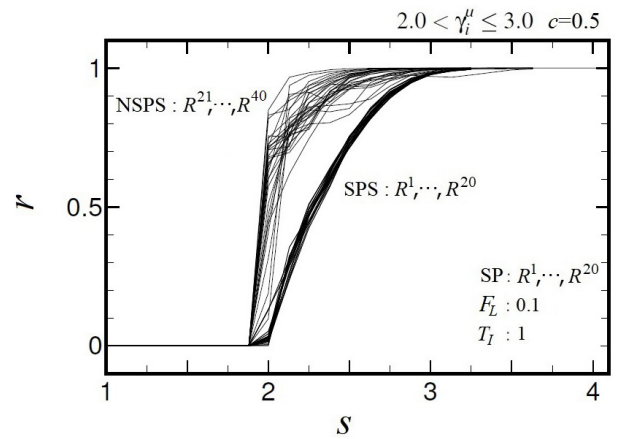


Fig. 9. Dependence of network response on signal strength when $M = 20$, $F_L = 0.1$ and $T_I = 1$ under the condition of $2.0 < \gamma_i^\mu \leq 3.0$ and $c = 0.5$.

tion was $1/8$). The dependence on the signal strength is shown in **Fig. 8** as a plot of each obtained value against s . In the interval where s is smaller than 2.0, the network resides in the nearest local equilibrium state (which is far from the input pattern information) and thus does not reflect the input information ($r = 0$). When the value of s exceeds 2.0, it becomes possible for the network to escape the local equilibrium state near the initial state, and it is led into a state close to the input signal. Also, due to the difference between the gradients of the energy function for the network states corresponding to stored and non-stored signals, the network responses for the two groups of signals differ considerably. The difference is maintained up to about $s = 2.5$, which indicates that it is possible to distinguish between stored and non-stored signals in this interval.

Similarly to **Fig. 8**, **Fig. 9** presents the dependence on the signal strength for all stored pattern signals (R^1, \dots, R^{20}) and the same number of non-stored pattern signals (R^{21}, \dots, R^{40}), where the fluctuation level F_L is set to 0.1.

Although the variance of the value of r corresponding to the group of non-stored pattern signals is somewhat prominent, in the interval $2.0 < s < 2.5$, there keeps a considerable difference between the respective network responses for stored and non-stored signals, which clearly indicates that it is possible to distinguish between stored and non-stored signals in this interval.

5. Evaluation of Pattern Discrimination Performance

5.1. Discrimination Method and Accuracy

In evaluating the pattern discrimination performance of the dynamic memory model, we focused on the difference between the dependence of the temporal correlation r on the signal strength for stored and non-stored signals as shown in **Fig. 9**, and we conducted the evaluation by determining whether a signal was stored or non-stored. Here, taking the dependence of the value of r corresponding to R^1 on s as the basis, we compared the dependence of r on s with respect to each input signal (R^n). Since the response curves of the stored patterns are all very similar, as can be seen from **Fig. 9**, the choice of any stored pattern as a basis has little effect on the experimental results. Specifically, for each s , we calculated the difference $\Delta r(s) (= r_{R^n}(s) - r_{R^1}(s))$ between the values of r corresponding to each input signal (R^n) and that of the SPS R^1 , after which we determined whether the signal is stored by checking whether the maximum $\Delta r_{\max} (= \max_s \{\Delta r(s)\})$ does not exceed a predetermined signal discrimination threshold Δr_{th} . Subsequently, we used the results to obtain the following formula for the accuracy P , which was regarded as a performance evaluation index [16].

$$P = \frac{n_s + n_{ns}}{2M} \quad (14)$$

Here, n_s (n_{ns}) is the number of stored (non-stored) patterns identified correctly as stored (non-stored).

Figure 10 presents the accuracy P for each signal discrimination threshold Δr_{th} . The accuracy is 1 ($P = 1$) for Δr_{th} in the interval between 0.15 and 0.4, which shows that stored signals are reliably distinguished from non-stored ones. The value of P decreases for small values of Δr_{th} , where Δr_{\max} of the stored signals exceeds Δr_{th} and they are misinterpreted as non-stored signals, as well as for large values of Δr_{th} , where Δr_{\max} of the non-stored signals does not exceed Δr_{th} and they are misinterpreted as stored signals.

5.2. Dependence of Signal Discrimination Performance on Fluctuation Level

Similar to the case of $F_L = 0.1$ in **Fig. 10**, **Fig. 11** shows P corresponding to Δr_{th} for each value of $F_L = 0.1, 0.2, 0.4, 0.6, 0.8$. The signal discrimination performance increases together with the fluctuation level and reaches a maximum at $F_L = 0.4$. There, the interval of

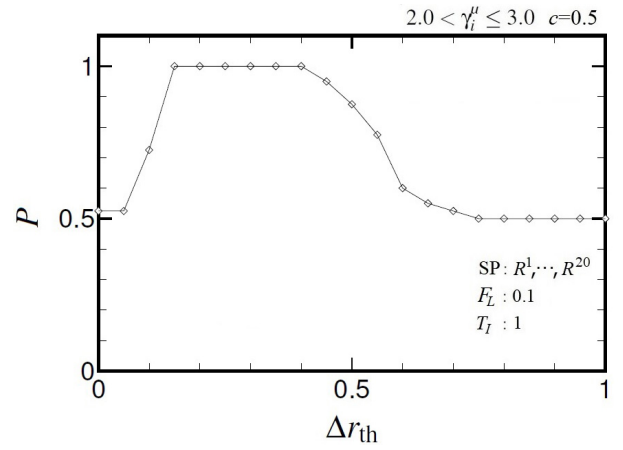


Fig. 10. Dependence of accuracy rate on discrimination threshold value when $M = 20$, $F_L = 0.1$, and $T_I = 1$ under the condition of $2.0 < \gamma_i^\mu \leq 3.0$ and $c = 0.5$.

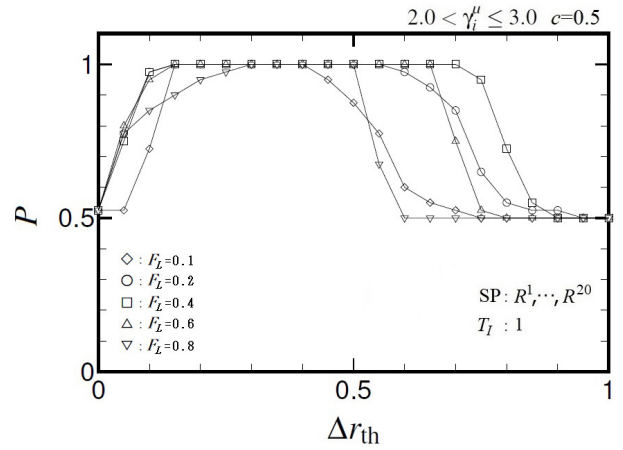


Fig. 11. Dependence of accuracy on discrimination threshold value for each fluctuation level when $M = 20$ and $T_I = 1$ under the condition of $2.0 < \gamma_i^\mu \leq 3.0$ and $c = 0.5$.

Δr_{th} in which stored signals can be reliably distinguished from non-stored ones (i.e., $P = 1$) is 0.15 to 0.7. When the fluctuation level exceeds 0.4, deterioration in the signal discrimination performance can be seen at higher threshold values as shown in $F_L = 0.6$ and 0.8. **Fig. 12** presents the interval for Δr_{th} in which the accuracy is 1 ($P = 1$) for each fluctuation level. For a wide interval of $\Delta r_{\text{th}} = 0.2$ to 0.6, the signal discrimination performance is reliable with $F_L = 0.3$ to 0.7.

The reason why the performance is influenced by the fluctuation level is that the influence of the gradient of the energy function is averaged over the space of network states corresponding to a fluctuation of 0 to F_L . **Figs. 13** and **14** show the results of a similar evaluation of the dependence on the signal strength as in **Fig. 9**, with the exception that the fluctuation level F_L is set to 0.4 and 0.8, respectively. In **Figs. 13** and **14**, the variance of r corresponding to each non-stored signal decreases, and the difference in network response for the two groups of stored and non-stored patterns becomes steadier, compared to

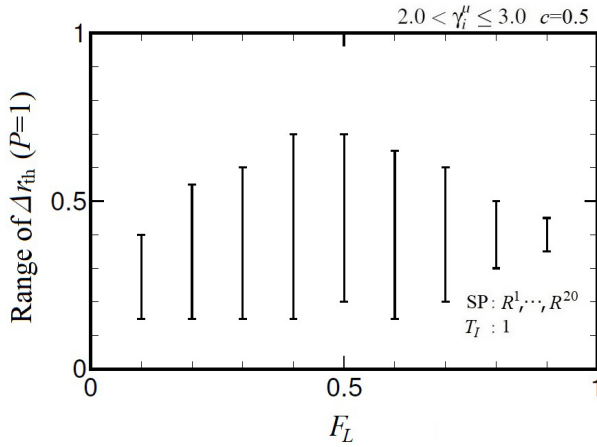


Fig. 12. Range of perfect discrimination ($P = 1$) threshold value versus fluctuation level in $M = 20$ and $T_I = 1$ under the condition of $2.0 < \gamma_i^\mu \leq 3.0$ and $c = 0.5$.

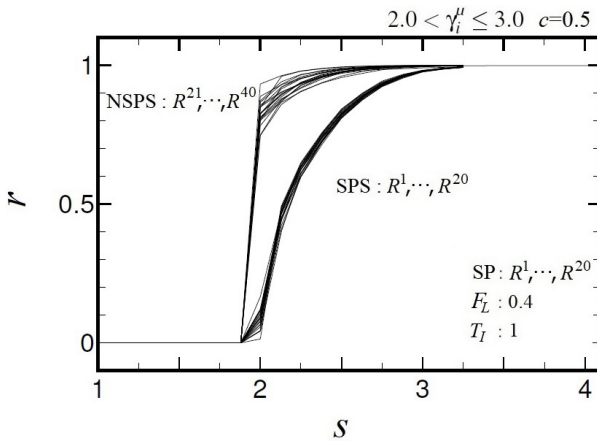


Fig. 13. Dependence of network response on signal strength when $M = 20$, $F_L = 0.4$, and $T_I = 1$ under the condition of $2.0 < \gamma_i^\mu \leq 3.0$ and $c = 0.5$.

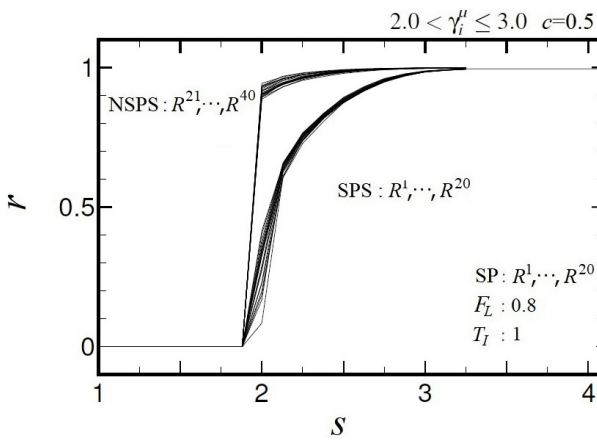


Fig. 14. Dependence of network response on signal strength when $M = 20$, $F_L = 0.8$, and $T_I = 1$ under the condition of $2.0 < \gamma_i^\mu \leq 3.0$ and $c = 0.5$.

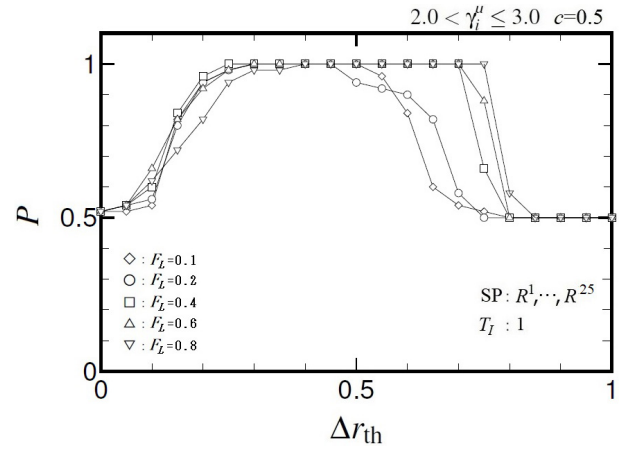


Fig. 15. Dependence of accuracy on discrimination threshold value for each fluctuation level when $M = 25$ and $T_I = 1$ under the condition of $2.0 < \gamma_i^\mu \leq 3.0$ and $c = 0.5$.

the case in **Fig. 9**. In this way, the averaging interval in accordance with F_L can be linked to the extraction of the characteristic gradient relation between stored and non-stored states.

5.3. Dependence of Signal Discrimination Performance on the Number of Memorized Patterns

Next, we evaluate the signal discrimination performance with regard to the number of memorized patterns. When the number of memorized patterns is 25 ($M = 25$), we evaluated the accuracy P corresponding to the signal discrimination threshold Δr_{th} with respect to each value of F_L for all input patterns (stored: R^1, \dots, R^{25} , non-stored: R^{26}, \dots, R^{50}); the results are presented in **Fig. 15**. Compared with the result in the case of $M = 20$ in **Fig. 11**, there is a tendency that the Δr_{th} dependence of the P value shifts to the higher value side of Δr_{th} , and the deterioration of the signal discrimination performance against the region close to $P = 1$ is small. Furthermore, even when the fluctuation level exceeded 0.4, there was no sudden deterioration of the signal discrimination performance, and an upper limit for Δr_{th} which displays high signal discrimination performance was maintained.

Figure 16 shows the interval for Δr_{th} in which the accuracy is 1 ($P = 1$) for each fluctuation level. Although deterioration is seen as compared with the case of $M = 20$, reliable signal discrimination performance is maintained in the interval of $F_L = 0.3$ to 0.7 with the almost same range of discrimination threshold Δr_{th} . In addition, a threshold width providing perfect discrimination performance is maintained in about 0.3 even for large values of $F_L = 0.8$ and 0.9.

Figure 17 shows the results of evaluating the differences in signal discrimination performance with respect to the number of memorized patterns. Although the signal discrimination performance deteriorates following the increase in the number of memorized patterns, reliable dis-

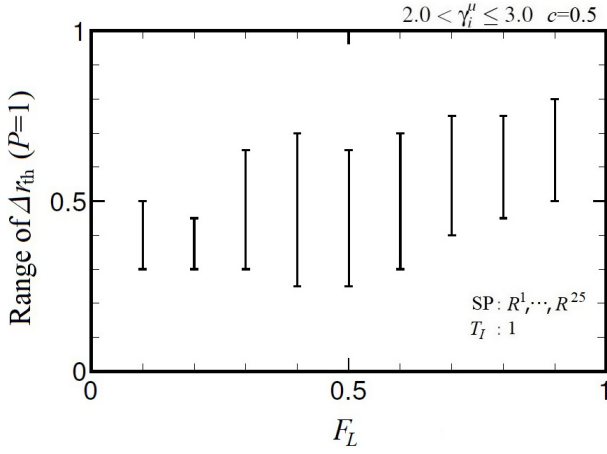


Fig. 16. Range of perfect discrimination ($P = 1$) threshold values versus fluctuation level when $M = 25$ and $T_I = 1$ under the condition of $2.0 < \gamma_i^\mu \leq 3.0$ and $c = 0.5$.

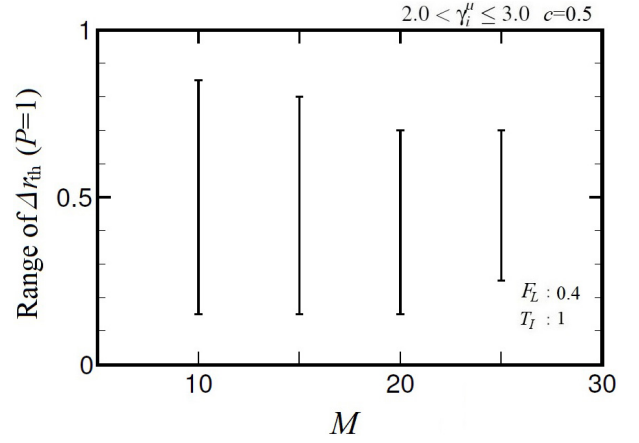


Fig. 18. Range of perfect discrimination ($P = 1$) threshold value versus the number of stored patterns when $F_L = 0.4$ and $T_I = 1$ under the condition of $2.0 < \gamma_i^\mu \leq 3.0$ and $c = 0.5$.

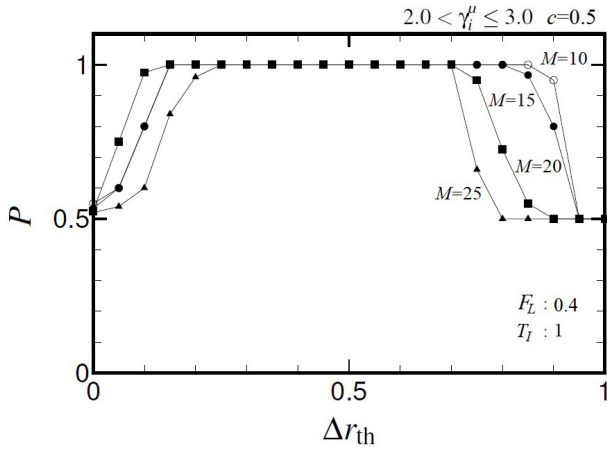


Fig. 17. Dependence of accuracy on discrimination threshold value for various numbers of stored patterns when $F_L = 0.4$ and $T_I = 1$ under the condition of $2.0 < \gamma_i^\mu \leq 3.0$ and $c = 0.5$.

crimination performance is maintained in the wide interval of $\Delta r_{th} = 0.25$ to 0.7 . **Fig. 18** shows the interval for Δr_{th} in which the accuracy with respect to the number of memorized patterns is 1 ($P = 1$). If the signal discrimination threshold Δr_{th} is taken in the interval of 0.25 to 0.7 , for input signals with $F_L = 0.4$, reliable pattern discrimination performance can be maintained for stored and non-stored signals regardless of any increase in the number of stored patterns (up to $M = 25$).

6. Conclusion

In this paper, we extended the static memory model based on Hopfield neural networks into a dynamic memory model capable of interacting with external signals. We performed a detailed analysis of its performance in terms of distinguishing between stored and non-stored patterns by evaluating its accuracy with respect to the number of

memorized patterns, the fluctuation level of the signal and the signal discrimination threshold. As a result, we discovered that the network response to stored and non-stored pattern signals differed considerably with respect to its dependence on the signal strength, and we confirmed that an allowable interval for the signal discrimination threshold was obtained in which the accuracy was high ($P = 1$).

In addition, the allowable interval for the signal discrimination threshold tended to expand if the input pattern signals were characterized by fluctuation, and by analyzing its dependence on the fluctuation level, we discovered that reliable signal discrimination ($P = 1$) was possible within a wide interval without the need for fine-tuning of the fluctuation level. Also, although the allowable interval for the signal discrimination threshold tended to become narrower following the increase of the number of memorized patterns, reliable discrimination performance ($P = 1$) was maintained, thus demonstrating the effectiveness of the proposed model.

Tasks that remain for future research include the exploration of methods for extending the network size in order to maintain high discrimination performance with respect to a substantial increase of the number of memorized patterns. Specifically, it is necessary to analyze the relation between the memorization ratio ((number of memorized patterns M)/(total number of neurons N)) and the allowable interval for the signal discrimination threshold. We will also apply this model to more practical problems, such as identification of personal records based on facial image data. Another future development will be the evaluation of the signal discrimination performance under the chaotic fluctuation emerged in chaotic neural networks.

Finally, it is also interesting to implement our dynamic scheme in associative memory networks with spiking neurons [21,22]. In this paper, we have proposed this scheme with the aim of practical information utilization, but we think that there may be room for examination of the possibility as a neuroscientific modeling in the actual brain.

Then, the setting of the discrimination mechanism in the brain which is compatible with the neuroscientific intuition, which replaces the correlation coefficient between input and output signals introduced in this study, becomes an important problem.

References:

- [1] J. J. Hopfield, "Neural networks and physical systems with emergent collective computational abilities," *Proc. of the National Academy of Sciences of the United States of America*, Vol.79, No.8, pp. 2554-2558, 1982.
- [2] J. J. Hopfield, "Neurons with graded response have collective computational properties like those of two-state neurons," *Proc. of the National Academy of Sciences of the United States of America*, Vol.81, pp. 3088-3092, 1984.
- [3] S. S. Haykin, "Neural Networks: A Comprehensive Foundation," Macmillan USA, 1994.
- [4] B. Müller and J. Reinhardt, "Neural Networks: An Introduction," Springer-Verlag, Berlin Heidelberg, 1995.
- [5] M. K. Müezzinoğlu, C. Güzelış, and J. M. Zurada, "An energy function-based design method for discrete Hopfield associative memory with attractive fixed points," *IEEE Trans. on Neural Networks*, Vol.16, No.2, pp. 370-378, 2005.
- [6] G. Pajares, "A Hopfield Neural Network for Image Change Detection," *IEEE Trans. on Neural Networks*, Vol.17, No.5, pp. 1250-1264, 2006.
- [7] R. Kruse, S. Mostaghim, C. Borgelt, C. Braune, and M. Steinbrecher, "Hopfield networks" in "Computational Intelligence," Springer, London, 2016.
- [8] K. Aihara, T. Takabe, and M. Toyoda, "Chaotic neural networks," *Phys. Lett. A*, Vol.144, No.6, pp. 333-340, 1990.
- [9] M. Adachi and K. Aihara, "Associative dynamics in a chaotic neural network," *Neural Network*, Vol.10, No.1, pp. 83-98, 1997.
- [10] M. Riani and E. Simonotto, "Stochastic resonance in the perceptual interpretation of ambiguous figures: A neural network model," *Phys. Rev. Lett.*, Vol.72, No.19, pp. 3120-3123, 1994.
- [11] N. Katada and H. Nishimura, "Stochastic resonance in recurrent neural network with Hopfield-type memory," *Neural Process. Lett.*, Vol.30, pp. 145-154, 2009.
- [12] H. Nishimura, N. Katada, and Y. Fujita, "Dynamic learning and retrieving scheme based on chaotic neuron model," E. R. Nakamura et al. (Eds.), "Complexity and Diversity," pp. 64-66, Springer-Verlag, Tokyo, 1997.
- [13] H. Nishimura and N. Katada, "Dynamic learning characteristics of chaotic neural networks with stimulus-response scheme," *Trans. of the Institute of Systems, Control and Information Engineers*, Vol.10, No.10, pp. 518-527, 1997 (in Japanese).
- [14] H. Nishimura, N. Katada, and K. Aihara, "Coherent response in a chaotic neural network," *Neural Process. Lett.*, Vol.12, pp. 49-58, 2000.
- [15] H. Nishimura, H. Doho, and N. Katada, "Signal recognition by input-output correlation in associative neural networks," *Electronics and Communications in Japan (Part III: Fundamental Electronic Science)*, Vol.86, Issue 5, pp. 54-64, 2003.
- [16] H. Doho, H. Nishimura, and N. Katada, "Dynamic pattern recognition model based on the characteristics of neural network response to signal fluctuation," *Proc. of 18th Fuzzy, Artificial Intelligence, Neural Networks and Computational Intelligence*, pp. 491-496, 2008 (in Japanese).
- [17] C. M. Marcus and R. M. Westervelt, "Dynamics of iterated-map neural networks," *Phys. Rev. A*, Vol.40, No.1, pp. 501-504, 1989.
- [18] P. Koiran, "Dynamics of discrete time continuous state Hopfield networks," *Neural Computation*, Vol.6, No.3, pp. 459-468, 1994.
- [19] S. Diederich and M. Oppen, "Learning of correlated patterns in spin-glass networks by local learning rules," *Phys. Rev. Lett.*, Vol.58, No.9, pp. 949-952, 1987.
- [20] D. O. Hebb, "The Organization of Behavior," Wiley, New York, 1949.
- [21] N. Hiratani, J. Teramae, and T. Fukai, "Associative memory model with long-tail-distributed Hebbian synaptic connections," *Front Comput. Neuroscience*, Vol.6, 2013. <https://doi.org/10.3389/fncom.2012.00102>
- [22] W. Gerstner, W. M. Kistler, R. Naud, and L. Paninski, "Memory Networks with Spiking Neurons, Neuronal Dynamics: From Single Neurons to Networks and Models of Cognition," Cambridge University Press, 2014.



Name:

Hiroataka Doho

Affiliation:

Professor, Faculty of Education, Kochi University

Address:

2-5-1 Akebono-cho, Kochi 780-8520, Japan

Brief Biographical History:

2007-2012 Associate Professor, Kochi University

2012- Professor, Kochi University

2022 Received Ph.D. degree in Applied Informatics from University of Hyogo

Main Works:

- H. Doho, S. Nobukawa, H. Nishimura, N. Wagatsuma, and T. Takahashi, "Transition of Neural Activity from the Chaotic Bipolar-Disorder State to the Periodic Healthy State Using External Feedback Signals," *Frontiers in Computational Neuroscience*, Vol.14, 2020. <https://doi.org/10.3389/fncom.2020.00076>
- S. Nobukawa, H. Doho, N. Shibata, H. Nishimura, and T. Yamanishi, "Chaos-Chaos Intermittency Synchronization Controlled by External Feedback Signals in Chua's Circuit," *IEICE Trans. on Fundamentals of Electronics, Communications and Computer Sciences*, Vol.E103.A, No.1, pp. 303-312, 2020.
- K. Nagano and H. Doho, "Development of Teaching Materials for Measurement and Control Configurable Various Systems Considering Instructions on Computers and Interfaces," *J. of the Japan Society of Technology Education*, Vol.63, No.2, pp. 197-206, 2021 (in Japanese).

Membership in Academic Societies:

- The Institute of Electronics, Information and Communication Engineers (IEICE)
- The Society of Instrument and Control Engineers (SICE)
- The Institute of Systems, Control and Information Engineers (ISCIE)
- Japan Society of Technology Education (JSTE)



Name:
Haruhiko Nishimura

ORCID:
0000-0003-1572-6747

Affiliation:
Specially Appointed Professor and Emeritus
Professor, Graduate School of Applied Informatics,
University of Hyogo

Address:

Computational Science Center BLDG., 7-1-28 Minatojima-Minami-cho,
Chuo-ku, Kobe 650-0047, Japan

Brief Biographical History:

1980 Graduated from Department of Physics, Shizuoka University
1985 Received Ph.D. degree from Kobe University
1989- Faculty of Medicine, Hiroshima University
1990- Associate Professor, Hyogo University of Education
1999- Professor, Hyogo University of Education
2004- Professor, University of Hyogo

Main Works:

- Intelligent systems science based on several architectures such as neural networks and complex systems, biomedical, healthcare, and high-confidence sciences.

Membership in Academic Societies:

- Institute of Electrical and Electronics Engineers (IEEE)
- The Institute of Electronics, Information and Communication Engineers (IEICE)
- Information Processing Society of Japan (IPSJ)
- Japanese Neural Network Society (JNNS)



Name:
Sou Nobukawa

ORCID:
0000-0001-7003-6912

Affiliation:
Professor, Department of Computer Science,
Chiba Institute of Technology

Address:

2-17-1 Tsudanuma, Narashino, Chiba 275-0016, Japan

Brief Biographical History:

2013-2014 Assistant Professor, University of Hyogo
2014-2016 Lecturer, Fukui University of Technology
2016-2017 Associate Professor, Fukui University of Technology
2017-2022 Associate Professor, Chiba Institute of Technology
2022- Professor, Chiba Institute of Technology

Main Works:

- S. Nobukawa, H. Nishimura, N. Wagatsuma, S. Ando, and T. Yamanishi, "Long-tailed characteristic of spiking pattern alternation induced by log-normal excitatory synaptic distribution," IEEE Trans. on Neural Networks and Learning Systems, Vol.32, No.8, pp. 3525-3537, 2021.
- S. Nobukawa, M. Kikuchi, and T. Takahashi, "Changes in functional connectivity dynamics with aging: A dynamical phase synchronization approach," NeuroImage, Vol.188, pp. 357-368, 2019.
- S. Nobukawa, H. Nishimura, and T. Yamanishi, "Chaotic resonance in typical routes to chaos in the Izhikevich neuron model," Scientific Reports, Vol.7, Article No.1331, 2017.

Membership in Academic Societies:

- Institute of Electrical and Electronics Engineers (IEEE)
- International Neural Network Society (INNS)
- The Institute of Electronics, Information and Communication Engineers (IEICE)
- Information Processing Society of Japan (IPSJ)
- The Society of Instrument and Control Engineers (SICE)
- The Institute of Systems, Control and Information Engineers (ISCIE)